



Published in final edited form as:

*J Neurosci Methods*. 2008 July 15; 172(1): 8–12. doi:10.1016/j.jneumeth.2008.04.001.

## Measuring *N*-acetyl aspartate synthesis *in vivo* using proton magnetic resonance spectroscopy

Su Xu, Jehoon Yang, and Jun Shen

Molecular Imaging Branch, National Institute of Mental Health, Bethesda, MD 20892, USA

### Abstract

*N*-acetyl aspartate (NAA) is an important marker of neuronal function and viability that can be measured using magnetic resonance spectroscopy (MRS). In this paper, we proposed a method to measure NAA synthesis using proton MRS with infusion of uniformly  $^{13}\text{C}$ -labeled glucose, and demonstrated its feasibility in an *in vivo* study of the rat brain. The rate of  $^{13}\text{C}$ -label incorporation into the acetyl group of NAA was measured using a localized, long echo-time proton MRS method. Signals from the  $^{13}\text{C}$  satellites of the main NAA methyl protons at 2.02 ppm were continuously monitored for 10 hours. Quantification of the data based on a linear kinetic model showed that NAA synthesis rate in isoflurane-anesthetized rats was  $0.19 \pm 0.02 \mu\text{mol/g/h}$  (mean  $\pm$  standard deviation,  $n = 12$ ).

### Keywords

*N*-acetyl aspartate synthesis; proton magnetic resonance spectroscopy; *in vivo*

### Introduction

*N*-acetyl aspartate (NAA) is found in high concentration ( $\sim 10 \mu\text{mol/g}$ ) exclusively in the nervous system (Tallan, 1957; Miyake et al., 1981; Koller et al., 1984; Pan et al., 2005). It is primarily synthesized from acetyl coenzyme A (acetyl-CoA) and aspartate by NAA synthase (L-aspartate *N*-acetyltransferase; ANAT, EC 2.3.1.17) in neuronal mitochondria, or via cleaving *N*-acetylaspartylglutamate (NAAG) catalyzed by *N*-acetylated- $\alpha$ -linked-amino dipeptidase (NAALADase) along with glutamate, and subsequently exported to the cytoplasm (Patel et al., 1979, Bzdega et al. 1997, Luthi-Carter et al., 1998). The major NAA catabolic enzyme aspartoacylase (*N*-acetylaspartate amidohydrolase; EC 3.5.1.15) is located in oligodendrocytes (Kaul et al., 1991; Baslow et al., 1999). NAA has been widely used as a neuronal marker in the study of a variety of cerebral disorders using *in vivo* proton magnetic resonance spectroscopy (MRS) (see Moffett et al., 2007 for a recent review). Abnormalities in NAA synthesis, transport and/or breakdown may contribute to abnormal steady state NAA concentrations observable in proton MRS spectra of the brain (Clark, 1998; Moreno et al., 2001). Canavan disease, for example, is an NAA metabolic disorder due to *N*-aspartoacylase deficiency which results in elevation of the NAA signal in proton MRS spectra (Kvittingen et al., 1986; Matalon et al., 1988; Burns et al., 1992; Moreno et al., 2001). In contrast to the large

Address correspondence to: Jun Shen, Ph. D., Molecular Imaging Branch, National Institute of Mental Health, Bldg. 10, Rm. 2D51A, 9000 Rockville Pike, Bethesda, MD 20892-1527, Tel.: (301) 451-3408, Fax: (301) 480-2397, Email: shenj@intra.nimh.nih.gov.

**Publisher's Disclaimer:** This is a PDF file of an unedited manuscript that has been accepted for publication. As a service to our customers we are providing this early version of the manuscript. The manuscript will undergo copyediting, typesetting, and review of the resulting proof before it is published in its final citable form. Please note that during the production process errors may be discovered which could affect the content, and all legal disclaimers that apply to the journal pertain.

body of literature on the total concentration of NAA in various brain disorders, the characterization of NAA synthesis remains scarce. Because NAA synthesis is dependent on mitochondrial metabolism and glucose is the major energy source of the brain under most conditions,  $^{14}\text{C}$  and  $^{13}\text{C}$  labeled glucoses have been used as primary substrates to determine the rate of NAA synthesis ( $V_{\text{NAA}}$ ) (Fig. 1). Using an *in vitro* enzymatic method, the activity of ANAT in adult rat brain homogenates was determined to be 0.19–0.58  $\mu\text{mol/g/h}$  depending on specific brain anatomy. The cortex activity was found to be 0.29  $\mu\text{mol/g/h}$  by Truckenmiller et al (1985). The activity of ANAT in the forebrain homogenate of thirty-five day old rats was determined to be 0.72  $\mu\text{mol/g/h}$  (Burri et al., 1991). The *in vivo* cerebral  $V_{\text{NAA}}$  has been directly measured using  $^{13}\text{C}$  MRS in both  $\alpha$ -chloralose-anesthetized adult rats ( $V_{\text{NAA}} = 0.7 \pm 0.1 \mu\text{mol/g/h}$ ) (Choi and Gruetter, 2004) and humans ( $V_{\text{NAA}} = 0.55 \pm 0.23 \mu\text{mol/g/h}$ ) (Moreno et al., 2001).

The direct  $^{13}\text{C}$  methods are limited by the inherently low sensitivity of  $^{13}\text{C}$  MRS. The *N*-acetyl methyl group of NAA is the major resonance in water-suppressed proton MRS spectra. The three magnetically equivalent hydrogen atoms of the methyl group resonate in proton MRS spectra with a single, sharp peak at 2.02 ppm, and therefore NAA has been generally recognized as one of the most reliable markers in brain MRS studies (Fan et al., 1986; Luyten and den Hollander, 1986; Barany et al., 1987). Because of the prominence of the NAA proton signal in MRS and its significantly higher sensitivity compared to  $^{13}\text{C}$ -labeled metabolite signals, a potentially useful approach is to determine NAA synthesis by measuring the  $^{13}\text{C}$  satellite signals of NAA in the proton MRS spectra. The resonances of the  $^{13}\text{C}$  satellite peaks are symmetrically located with respect to the central resonance of the methyl protons attached to  $^{12}\text{C}$ . The intensity ratio of the satellite peaks to the total NAA signal reveals the  $^{13}\text{C}$  isotopic enrichment of the acetyl moiety of NAA. Unlike direct  $^{13}\text{C}$  methods which require a radio frequency (RF) coil tuned to  $^{13}\text{C}$  nuclei and a second RF channel as well as broadband amplifiers, proton MRS is in principle available on all clinical scanners, and by far the most widely used MRS technique. In this study, we demonstrate that  $V_{\text{NAA}}$  can be measured *in vivo* using a localized long echo-time (TE) proton MRS method with infusion of uniformly  $^{13}\text{C}$ -labeled glucose ( $[\text{U-}^{13}\text{C}]\text{glucose}$ ) to label the *N*-acetyl methyl group of NAA without using a  $^{13}\text{C}$  channel. A similar approach for measuring the  $^{13}\text{C}$  labeling of glutamate was previously reported (Boumezbeur et al., 2004).

## Materials and Methods

Male young adult Sprague-Dawley rats (169–217 g,  $n = 12$ ) were fasted overnight (> 12 hours) with free access to drinking water. For preparation, the rats were anaesthetized with isoflurane (1.5%) in a mixture of 70%  $\text{N}_2\text{O}/30\% \text{O}_2$ . The left femoral artery was cannulated for periodically sampling of arterial blood to monitor blood gases ( $\text{pO}_2$ ,  $\text{pCO}_2$ ), pH, and glucose concentration using a blood analyzer (Bayer Rapidlab 860, East Walpole, MA), and for monitoring arterial blood pressure levels. The left femoral vein was also cannulated for intravenous infusion of  $[\text{U-}^{13}\text{C}]\text{glucose}$  (99% enrichment, Cambridge Isotope Labs, Andover, MA, 20 % wt/vol). The glucose infusion protocol consisted of an initial bolus of 162 mg/kg/min of 1.1 M  $[\text{U-}^{13}\text{C}]\text{glucose}$  in the first ten minutes followed by an approximately constant infusion rate of 62.8 mg/kg/min. Plasma glucose level was maintained at  $19.6 \pm 1.6 \text{ mM}$  during the experiment. Arterial blood  $\text{pO}_2$ ,  $\text{pCO}_2$ , mean blood pressure, and pH were maintained at approximately  $129 \pm 16 \text{ mm Hg}$ ,  $36 \pm 4 \text{ mmHg}$ ,  $100\text{--}145 \text{ mm Hg}$ , and  $7.34 \pm 0.04$ , respectively. All procedures were approved by the National Institute of Mental Health Animal Care and Use Committee.

The *in vivo* MRS experiments were performed on a Bruker 11.7 Tesla spectrometer interfaced to an 89 mm inner-diameter vertical bore magnet. A 15-mm inner diameter proton surface coil was used for excitation and detection, and was positioned  $\sim 0\text{--}1 \text{ mm}$  posterior to bregma.

Adjustment of all first- and second-order shims was accomplished using a fully automatic procedure described previously (Chen et al., 2004) which was based on a fast automatic shimming technique by mapping along projections method (Gruetter, 1993). The single-shot adiabatic 3D localization pulse sequence (Slotboom et al., 1991) was similar to that used in our previously study (Xu et al., 2005) but with a lengthened echo-time (TE = 100 ms). Specifically, the proton MRS pulse sequence used slice-selective adiabatic refocusing with two hyperbolic secant pulses per dimension (Conolly et al., 1991) (2 ms sech pulse,  $\mu = 5$ , 1% truncation). Chemical shift selective (CHESS) water suppression (Gueron et al., 1991) was used together with outer volume suppression using nominal 90° hyperbolic secant pulses along the  $x$  (10-mm slab),  $-x$  (10-mm slab),  $y$  (3-mm slab),  $-y$  (5-mm slab),  $z$  (10-mm slab), and  $-z$  (10-mm slab) directions. The CHESS and the outer volume suppression pulses were repeated three times. Orthogonal gradient pairs or triplets carefully adjusted to minimize the resultant  $B_0$  shifts were used as crushers for CHESS, outer volume suppression, and for the slice-selective refocusing adiabatic pulses. Proton MRS spectra were acquired from a  $6 \times 3 \times 6$  mm<sup>3</sup> voxel centered on the midline of the brain with 4096 data points, a spectral width of 4000 Hz, and a repetition time (TR) of 3.2 s. For each data block, 440 acquisitions were accumulated over 24 minutes. After acquisition of each data block, a 6-minute interval was used for re-shimming to maintain  $B_0$  homogeneity over a total experimental duration of 10 hours. Satellite NAA methyl peaks were analyzed using the MATLAB curve-fitting toolbox (The MathWorks, Inc., Natick, MA). Since NAAG cannot be reliably quantified, the total NAA signal (= NAA + NAAG) was used instead. To minimize interference from the glutamate and glutamine H3 methylene group at 2.09 – 2.14 ppm regions, the upfield NAA satellite peak at 1.89 ppm was used in the quantification of <sup>13</sup>C-labeled NAA with its intensity multiplied by a factor of 2.

## Results

Fig. 2 shows examples of the localized ( $6 \times 3 \times 6$  mm<sup>3</sup>) proton MRS spectra of a normal rat brain at short echo-time (Fig. 2a, TE = 15 ms) and at long echo-time (Fig. 2b, TE = 100 ms) without infusion of [U-<sup>13</sup>C]glucose. The accumulated FID of each data block was zero-filled to 16 K. Resolution-enhancing Lorentz-Gauss transformation (exponential broadening factor (lb) = -4 Hz, Gaussian broadening factor (gb) = 0.3) was applied before Fourier transform. The spectra were phased using zero-order phase only, without any baseline corrections. These *in vivo* spectra show high sensitivity and spectral resolution achieved at the high magnetic field strength of 11.7 T used in the current study. In Fig. 2, the spectral pattern of resonances between 0.8 and 4.0 ppm shows a strong dependence upon TE. The short echo-time spectrum (Fig. 2a) minimizes the signal-to-noise ratio (SNR) loss mostly by the spin-spin relaxation dephasing, phase and intensity abnormality due to evolution of homonuclear scalar couplings of weakly and strongly coupled resonances. However, the analysis of NAA satellite signals at short TE is complicated due to the broad baseline originating from macromolecules as well as overlapping resonances from glutamate and glutamine H3 methylene protons. As shown in Fig. 2b, at the longer TE of 100 ms interference from glutamate and glutamine H3 and macromolecules is minimized while the NAA resonance at 2.02 ppm still maintains a high SNR.

A typical time course of spectra showing dynamic <sup>13</sup>C-label incorporation into the *N*-acetyl methyl group of NAA (<sup>1</sup>J<sub>CH</sub> = 128 Hz) during [U-<sup>13</sup>C]glucose infusion from the  $6 \times 3 \times 6$  mm<sup>3</sup> (108 μL) voxel of an individual rat brain is illustrated in Fig. 3a (lb = -1Hz, gb = 0.005). The signal intensity of the NAA satellite peaks increased progressively as a function of time due to <sup>13</sup>C-label incorporation from C1 and C6 of [U-<sup>13</sup>C]glucose into NAA C6. Both [U-<sup>13</sup>C]glucose and [1,6-<sup>13</sup>C<sub>2</sub>]glucose produce two acetyl-CoA with <sup>13</sup>C labels at their C2 positions (and therefore at NAA C6), therefore doubling the SNR obtainable using [1-<sup>13</sup>C]glucose or [6-<sup>13</sup>C]glucose. Note that the simultaneous <sup>13</sup>C-label incorporation from C2 and C5 of [U-<sup>13</sup>C]glucose into NAA C5, which has a heteronuclear coupling of ~5 Hz to the methyl

protons of NAA, does not affect the measurement of  $V_{\text{NAA}}$ . The use of [U- $^{13}\text{C}$ ]glucose instead of [1,6- $^{13}\text{C}_2$ ]glucose is because the former is much less costly. The spectroscopy voxel used in this study is predominantly located in the rat neocortex as shown in a coronal anatomical image (Fig. 3b). Because the observed kinetics of  $^{13}\text{C}$ -label incorporation into the acetyl moiety of NAA was found to be approximately linear within the experimental time frame, the time course of  $^{13}\text{C}$  isotopic enrichment of the NAA methyl group,  $^{13}\text{C}$ -NAA (t), was modeled as a linear equation based on the work of Choi and Gruetter (2004):

$$^{13}\text{C} - \text{NAA}(t)/\text{NAA}_0 = 0.011 + V_{\text{NAA}} \cdot t \quad [1]$$

where  $\text{NAA}_0$  is the total concentration of NAA. The constant 0.011 accounts for the natural abundance signal of  $^{13}\text{C}$ -labeled NAA.  $\text{NAA}_0 = 9.9 \mu\text{mol/g}$  was converted from our previously reported NAA concentration in the same brain region (Xu et al., 2005) based on the reported brain tissue specific gravity (DiResta et al., 1991). The NAA synthesis rate  $V_{\text{NAA}}$  was subsequently determined using least-squares fitting of the measured time courses of the  $^{13}\text{C}$  isotopic enrichment of NAA to the above equation. The time courses of  $^{13}\text{C}$  isotopic enrichment from the twelve rats (expressed as mean and standard deviation) and the fit to the linear model are shown in Fig 4. The NAA synthesis rate was determined to be  $V_{\text{NAA}} = 0.19 \pm 0.02 \mu\text{mol/g/h}$  (mean  $\pm$  standard deviation,  $n = 12$ ).

## Discussion

In this study, we demonstrated that proton MRS without the use of a  $^{13}\text{C}$  channel (Boumezbeur et al. 2004) could be utilized for measuring the NAA synthesis rate *in vivo*. We performed measurements of  $^{13}\text{C}$ -label incorporation into the acetyl moieties of NAA in an 108  $\mu\text{L}$  volume in the rat brain with [U- $^{13}\text{C}$ ]glucose infusion for ten hours. The proton MRS-only method takes advantage of the high sensitivity of proton detection and additional spectral resolution rendered by the  $^{13}\text{C}$  satellite peaks when no heteronuclear decoupling is applied. Compared to direct  $^{13}\text{C}$  MRS, *in vivo* proton MRS is a much more sensitive method due to its large gyromagnetic ratio ( $^1\text{H}$ :  $26.8 \times 10^7 \text{ rads}^{-1}\text{T}^{-1}$  vs.  $^{13}\text{C}$ :  $6.7 \times 10^7 \text{ rads}^{-1}\text{T}^{-1}$ ). In  $^{13}\text{C}$  MRS studies, proton decoupling techniques are usually used for increasing spectral resolution and sensitivity. However, a double-tuned RF coil or a two-coil assembly and broadband amplifiers are required to perform direct  $^{13}\text{C}$  MRS with proton decoupling. In addition, two RF channels are needed for excitation at both  $^1\text{H}$  and  $^{13}\text{C}$  frequencies in direct  $^{13}\text{C}$  MRS methods. Therefore, the proton-only MRS technique significantly simplifies the hardware requirements for measuring the NAA synthesis rate *in vivo*.

Although NAA H3 signals at 2.50 and 2.70 ppm were detected in Fig. 2b, they are not useful for quantification of  $V_{\text{NAA}}$  because of their substantially low intensity compared to the methyl proton signal of NAA at 2.02 ppm. No useful  $^{13}\text{C}$  satellite signals of NAA H3 were found after adding the last time point from the twelve animals (data not shown).

Compared with the activity of ANAT measured from rat brain homogenates, the smaller  $V_{\text{NAA}}$  value determined *in vivo* from isoflurane-anesthetized rats in the current study suggests that NAA synthesis *in vivo* may be limited by substrate availability. The regulation of ANAT *in vivo* is still largely unknown (Arun et al., 2006). Since the  $V_{\text{max}}$ -like activity of ANAT measured from brain homogenates does not necessarily reflect  $V_{\text{NAA}}$  *in vivo* other explanations for the smaller *in vivo*  $V_{\text{NAA}}$  measured in this study are also possible. It is unknown if anesthesia required for *in vivo* MRS study of animals affects  $V_{\text{NAA}}$ . Current evidence suggests that depression of basal metabolism by anesthetics does not correlate with a reduced  $V_{\text{NAA}}$ . A significantly higher  $V_{\text{NAA}}$  was reported in the literature ( $0.7 \pm 0.1 \mu\text{mol/g/h}$ , Choi and Gruetter, 2004) when using direct  $^{13}\text{C}$  MRS methods with  $\alpha$ -chloralose-anesthetized rats, although  $\alpha$ -chloralose is known to produce a larger attenuation of cerebral metabolism. The discrepancy between our study and that of Choi and Gruetter therefore may be due to other differences in

experimental conditions. For example, the use of highly sensitive proton detection allowed us to place the spectroscopy voxel in mostly neocortical gray matter (Fig. 3b). In the Choi and Gruetter *in vivo*  $^{13}\text{C}$  MRS study, a much larger voxel ( $8.5 \times 6 \times 10 \text{ mm}^3$  or  $510 \mu\text{l}$ ) which included a large portion of white matter and subcortical tissues was used to increase the sensitivity of  $^{13}\text{C}$  MRS. Since in several subcortical tissue types the activity of ANAT is substantially higher than that in the cortex (Truckenmiller et al., 1985) and the activity of ANAT in white matter is yet to be determined, the large difference in voxel size between the Choi and Gruetter study and our study is expected to have contributed significantly to this apparent discrepancy.

Eq. [1] intrinsically assumes that the  $^{13}\text{C}$  fractional enrichment of the precursor acetyl-CoA is 100%. If the presence of neuronal isotope dilution is significant, the  $^{13}\text{C}$  fractional enrichment of the precursor acetyl-CoA is expected to be less than 100%. The presence of endogenous unlabeled glucose will also reduce the  $^{13}\text{C}$  fractional enrichment of acetyl-CoA. However, based on our previous study using the same infusion protocol the  $^{13}\text{C}$  fractional enrichment of blood glucose is very close to 100% (96%, Xu and Shen, 2006). Isotope dilution of neuronal acetyl-CoA is also expected to be insignificant due to prolonged infusion of a large amount of fully and uniformly labeled glucose. The overall effect of overestimating the isotopic enrichment of acetyl-CoA leads to underestimating  $V_{\text{NAA}}$ . Based on the above analysis, the underestimation of  $V_{\text{NAA}}$  due to incomplete labeling of the precursor neuronal acetyl-CoA pool is expected to be very small. It should also be pointed out that one important advantage of using proton MRS without heteronuclear decoupling is that the total NAA signal remains unchanged during the course of spectroscopy measurement and can be used as a concentration reference. In contrast, direct  $^{13}\text{C}$  MRS lacks an internal concentration reference and requires a more complicated quantification procedure.

Although the acetyl methyl proton peak of NAAG overlaps with that of NAA (see Fig. 2), NAAG has a much lower concentration in the brain ( $<0.5\text{--}1 \mu\text{mol/g}$ , Robinson et al. 1987, Fuhrman et al., 1994). More importantly, the turnover of NAAG catalyzed by NAALADase ( $\text{NAAG} \leftrightarrow \text{NAA} + \text{glutamate}$ ) is much more rapid, leading to an isotopic steady state between NAA and NAAG (Tyson and Sutherland, 1988). That is, NAA and NAAG have nearly the same  $^{13}\text{C}$  isotopic enrichment at the acetyl methyl carbon. Thus, Eq. [1] is valid when total NAA is used in lieu of NAA. Therefore, the presence of NAAG can be safely neglected during the measurement of  $V_{\text{NAA}}$ .

The current study was performed to explore the possibility of measuring NAA synthesis in human subjects using proton MRS. Although we used the high field strength of 11.7 Tesla and a voxel size of 0.1 ml, the sensitivity of proton MRS at clinically accessible field strength has been shown to be sufficient to detect natural abundance  $^{13}\text{C}$ -labeled NAA from human brain at a spatial resolution of 12 ml (Chen W, et al., 1998). Therefore, the isotopically enriched NAA  $^{13}\text{C}$  satellite signal is well above the sensitivity limit of clinical scanners. The spectral resolution is generally reduced at lower field strength. However, at long echo time, proton MRS spectra of brain at low field strength are known to be spectrally simplified, which can be taken advantage of to spectrally resolve the NAA  $^{13}\text{C}$  satellite signals.

In addition to the steady-state concentrations of NAA, NAA turnover rates in the human brain measured by direct  $^{13}\text{C}$  MRS methods have also been reported recently, offering an opportunity to better understand the role of NAA in brain metabolism and disorders of metabolism. The NAA synthesis rate was found to be approximately 60% lower in Canavan patients ( $0.56 \pm 0.23 \mu\text{mol/g/h}$  in controls versus  $0.22 \pm 0.01 \mu\text{mol/g/h}$  in Canavan disease) with a 50% increase in static NAA concentration (Moffett et al., 2007). In contrast to Canavan disease where NAA synthesis rate was reduced, NAA synthesis rates appeared to be modestly increased in patients with Alzheimer's disease (Harris et al., 2006). Our proton-only MRS strategy for detection of

NAA synthesis can be easily extended to lower field strength accessible to clinical research. Thus, with high sensitivity and easy implementation, the method proposed in this paper may provide potential applications to clinical studies of human brain disorders associated with abnormal NAA concentration and kinetics. It may also be used in measuring  $V_{\text{NAA}}$  in white matter and deep brain structures using a resonator or phased-array coil and in determining tissue-type specific  $V_{\text{NAA}}$ .

## References

- Arun P, Madhavarao CN, Moffett JR, Namboodiri MA. Regulation of N-acetylaspartate and N-acetylaspartylglutamate biosynthesis by protein kinase activators. *J Neurochem* 2006;98:2034–2042. [PubMed: 16945114]
- Barany M, Spigos DG, Mok E, Venkatasubramanian PN, Wilbur AC, Langer BG. High resolution proton magnetic resonance spectroscopy of human brain and liver. *Magn Reson Imaging* 1987;5:393–398. [PubMed: 2826962]
- Baslow MH, Suckow RF, Sapirstein V, Hungund BL. Expression of aspartoacylase activity in cultured rat macroglial cells is limited to oligodendrocytes. *J Mol Neurosci* 1999;13:47–53. [PubMed: 10691291]
- Boumezbeur F, Besret L, Valette J, Vaufrey F, Henry P, Slavov V, Giacomini E, Hantraye P, Bloch G, Lebon V. NMR measurement of brain oxidative metabolism in monkeys using  $^{13}\text{C}$ -labeled glucose without a  $^{13}\text{C}$  radiofrequency channel. *Magn Reson Med* 2004;52:33–40. [PubMed: 15236364]
- Burns S, Chalmers R, West R, Iles R. Measurement of human brain aspartate *N*-acetyl transferase flux *in vivo*. *Biochem Soc Trans* 1992;20:107S. [PubMed: 1397517]
- Burri R, Stefeen C, Herschkowitz N. *N*-acetyl-L-aspartate is a major source of acetyl groups for lipid synthesis during rat brain development. *Dev Neurosci* 1991;13:403–411. [PubMed: 1809557]
- Bzdega T, Turi T, Wroblewska B, She D, Chung HS, Kim H, Neale JH. Molecular cloning of a peptidase against N-acetylaspartylglutamate from a rat hippocampal cDNA library. *J Neurochem* 1997;69:2270–2277. [PubMed: 9375657]
- Chen W, Adriany G, Zhu XH, Gruetter R, Ugurbil K. Detecting natural abundance carbon signal of NAA metabolite within 12-cm<sup>3</sup> localized volume of human brain using  $^1\text{H}$ -[ $^{13}\text{C}$ ] NMR spectroscopy. *Magn Reson Med* 1998;40:180–184. [PubMed: 9702699]
- Chen Z, Li SS, Yang J, Letizia D, Shen J. Measurement and automatic correction of high-order  $B_0$  inhomogeneity in the rat brain at 11.7 Tesla. *Mag Reson Imag* 2004;2:835–842.
- Choi I, Gruetter R. Dynamic or inert metabolism? Turnover of *N*-acetyl aspartate and glutathione from D-[1- $^{13}\text{C}$ ]glucose in the rat brain *in vivo*. *J Neurochem* 2004;91:778–787. [PubMed: 15525331]
- Clark JB. *N*-acetyl aspartate: a marker for neuronal loss or mitochondrial dysfunction. *Dev Neurosci* 1998;20:271–276. [PubMed: 9778562]
- Conolly S, Glover G, Nishimura D, Macovski A. A reduced power selective adiabatic spin-echo pulse sequence. *Magn Reson Med* 1991;18:28–38. [PubMed: 2062239]
- DiResta GR, Lee JB, Arbit E. Measurement of brain tissue specific gravity using pycnometry. *J Neurosci Methods* 1991;39:245–251. [PubMed: 1787744]
- Fan TW, Higashi RM, Lane AN, Jardetzky O. Combined use of  $^1\text{H}$ -NMR and GC-MS for metabolite monitoring and *in vivo*  $^1\text{H}$ -NMR assignments. *Biochim Biophys Acta* 1986;882:154–167. [PubMed: 3011112]
- Fuhrman S, Palkovits M, Cassidy M, Neale JH. The Regional Distribution of *N*-Acetylaspartylglutamate (NAAG) and Peptidase Activity Against NAAG in the Rat Nervous System. *J Neurochem* 1994;62:275–281. [PubMed: 8263527]
- Gruetter R. Automatic, localized *in vivo* adjustment of all first- and second-order shim coils. *Magn Reson Med* 1993;29:804–811. [PubMed: 8350724]
- Gueron M, Plateau P, Decors M. Solvent signal suppression in NMR. *Progr NMR Spectrosc* 1991;23:135–209.
- Harris, K.; Lin, A.; Bhattacharya, P.; Tran, T.; Wong, W.; Ross, BD. Regulation of NAA-synthesis in the human grain *in vivo*: Canavan's disease, Alzheimer's disease and schizophrenia. In: Moffett, JR.; Tieman, SS.; Weinberger, DR.; Coyle, JT.; MA Namboodiri, MA., editors. *N*-Acetylaspartate: A

- Unique Naeronal Molecule in the Central Nervous Stsem. New York: Springer Science + Business Media; 2006. p. 263-273.
- Kaul R, Casanova J, Johnson AB, Tang P, Matalon R. Purification, characterization, and localization of aspartoacylase from bovine brain. *J Neurochem* 1991;56:129–135. [PubMed: 1987315]
- Koller KJ, Zaczek R, Coyle JT. *N*-acetyl-aspartyl-glutamate: regional levels in rat brain and the effects of brain lesions as determined by a new HPLC method. *J Neurochem* 1984;43:1136–1142. [PubMed: 6470709]
- Kvittingen E, Guldal G, Borsting S, Skalpe I, Stokke O, Jellum E. *N*-acetylaspartic aciduria in a child with a progressive cerebral atrophy. *Clin Chim Acta* 1986;158:217–227. [PubMed: 3769199]
- Luthi-Carter R, Berger UV, Barczak AK, Enna M, Coyle JT. Isolation and expression of a rat brain cDNA encoding glutamate carboxypeptidase II. *Proc Natl Acad Sci U S A* 1998;95:3215–3220. [PubMed: 9501243]
- Luyten PR, den Hollander JA. Observation of metabolites in the human brain by MR spectroscopy. *Radiology* 1986;161:795–798. [PubMed: 3786735]
- Matalon R, Michals K, Sebesta D, Deanching M, Gashkoff P, Casanova J. Aspartoacylase deficiency and *N*-acetylaspartic aciduria in patients with Canavan disease. *Am J Med Genet* 1988;29:463–471. [PubMed: 3354621]
- Miyake M, Kakimoto Y, Sorimachi M. A gas chromatographic method for the determination of *N*-acetyl-L-aspartic acid, *N*-acetyl- $\alpha$ -aspartylglutamic acid and beta-citryl-L-glutamic acid and their distributions in the brain and other organs of various species of animals. *J Neurochem* 1981;36:804–810. [PubMed: 7205274]
- Moffett JR, Ross B, Arun P, Madhavarao CN, Namboodiri AMA. *N*-Acetylaspartate in the CNS: from neurodiagnostics to neurobiology. *Prog Neurobiol* 2007;81:89–131. [PubMed: 17275978]
- Moreno A, Ross BD, Blüml S. Direct determination of the *N*-acetyl-L-aspartate synthesis rate in the human brain by  $^{13}\text{C}$  MRS and  $[1-^{13}\text{C}]$ glucose infusion. *J Neurochem* 2001;77:347–350. [PubMed: 11279290]
- Pan JW, Takahashi K. Interdependence of *N*-acetyl aspartate and high-energy phosphates in healthy human brain. *Ann Neurol* 2005;57:92–97. [PubMed: 15546136]
- Patel TB, Clark JB. Synthesis of *N*-acetyl-L-aspartate by rat brain mitochondria and its involvement in mitochondrial/cytosolic carbon transport. *Biochem J* 1979;184:539–546. [PubMed: 540047]
- Robinson MB, Blakely RD, Couto R, Coyle JT. Hydrolysis of the brain dipeptide *N*-acetyl-L-aspartyl-L-glutamate. Identification and characterization of a novel *N*-acetylated alpha-linked acidic dipeptidase activity from rat brain. *J Biol Chem* 1987;262:14498–14506. [PubMed: 3667587]
- Slotboom J, Mehlkopf AF, Bovee WMMJ. A single-shot localization pulse sequence suited for coils with inhomogeneous RF field using adiabatic slice-selective RF pulses. *J Magn Reson* 1991;95:396–404.
- Tallan HH. Studies on the distribution of *N*-acetyl-L-aspartic acid in brain. *J Boil Chem* 1957;224:41–45.
- Truckenmiller ME, Namboodiri MAA, Brownstein MJ, Neale JH. *N*-Acetylation of L-aspartate in the nervous system: differential distribution of a specific enzyme. *Neurochemistry* 1985;45:1658–1662.
- Tyson RL, Sutherland GR. Labeling of *N*-acetylaspartate and *N*-acetylaspartylglutamate in rat neocortex, hippocampus and cerebellum from  $[1-^{13}\text{C}]$ glucose. *Neurosci Lett* 1998;251:181–184. [PubMed: 9726373]
- Xu S, Yang J, Li CQ, Zhu W, Shen J. Metabolic alterations in focally activated primary somatosensory cortex of  $\alpha$ -chloralose-anesthetized rats measured by  $^1\text{H}$  MRS at 11.7 T. *NeuroImage* 2005;28:401–409. [PubMed: 16182571]
- Xu S, Shen J. *In vivo* dynamic turnover of cerebral  $^{13}\text{C}$  isotopomers from  $[U-^{13}\text{C}]$ glucose. *J Magn Reson* 2006;182:221–228. [PubMed: 16859940]

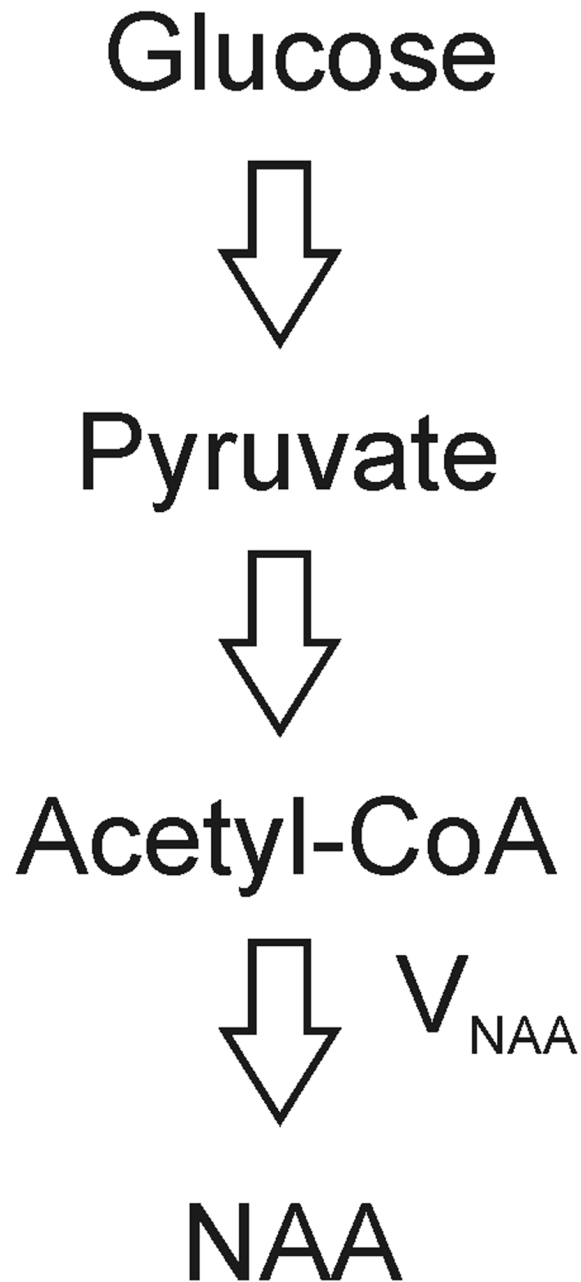


**Fig. 1.** Schematic representation of synthesis of NAA from glucose.  $V_{NAA}$ , NAA synthesis rate.



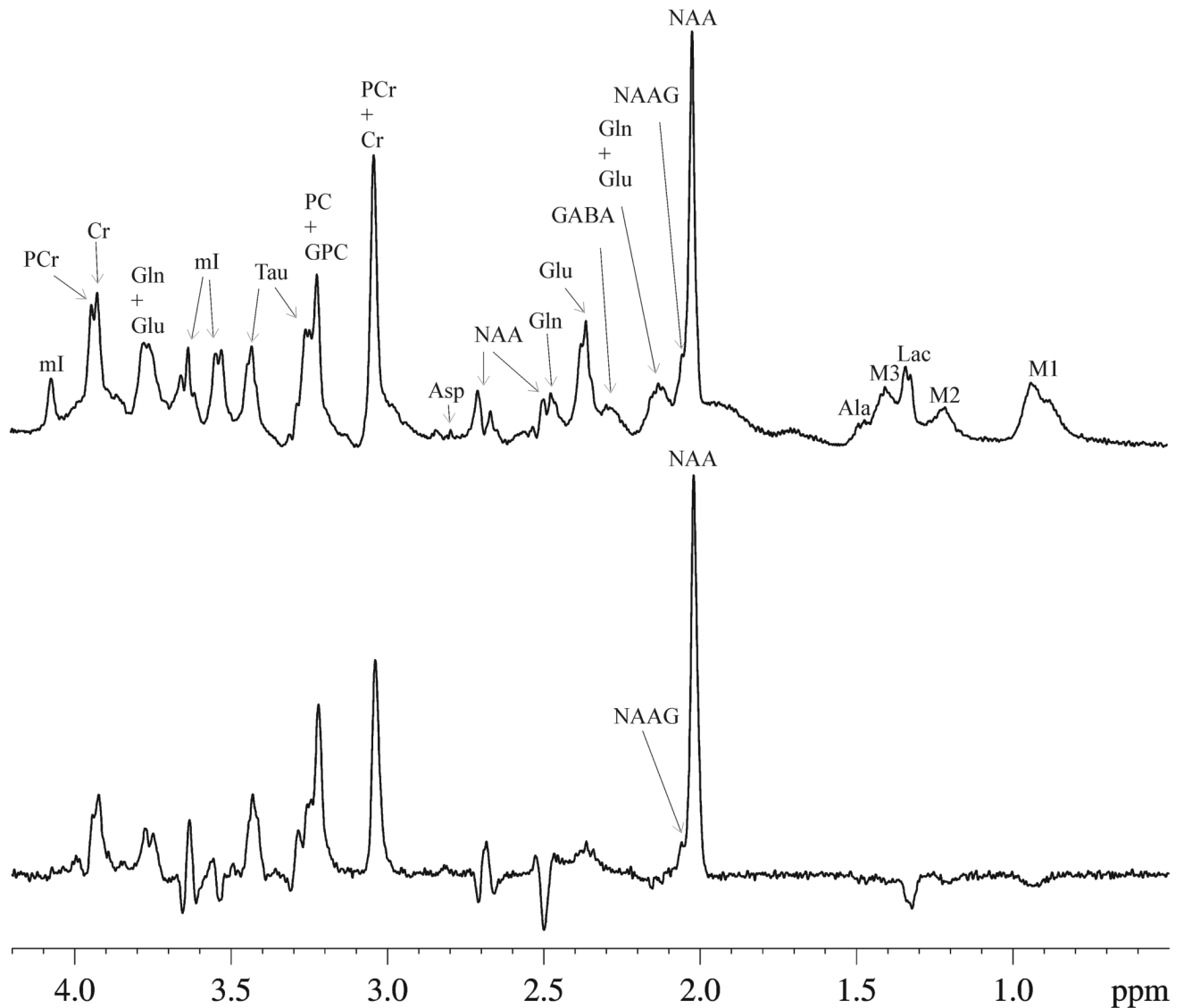


**Fig. 2.** The localized ( $6 \times 3 \times 6 \text{ mm}^3$ ) proton MRS spectra acquired from an individual rat brain with (a) short TE (TE = 15 ms, NA = 440, TR = 3.2 s, lb = -4 Hz, gb = 0.3) and (b) long TE (TE = 100 ms, NA = 1760, all other parameters were the same as in (a)). The spectra were phased using zero-order phase only without any baseline corrections, and were plotted using the same absolute intensity scale. Ala = alanine, Asp = aspartate, Cr = creatine, GABA =  $\gamma$ -aminobutyric acid, Gln = glutamine, Glu = glutamate, GPC = glycerophosphorylcholine, Lac = lactate, mI = myo-Inositol, NAA = *N*-acetylaspartate, NAAG = *N*-acetylaspartylglutamate, PC = phosphocholine, PCr = phosphocreatine, Tau = taurine, M1 = macromolecule at 0.92 ppm, M2 = macromolecule at 1.21 ppm, M3 = macromolecule at 1.39 ppm.

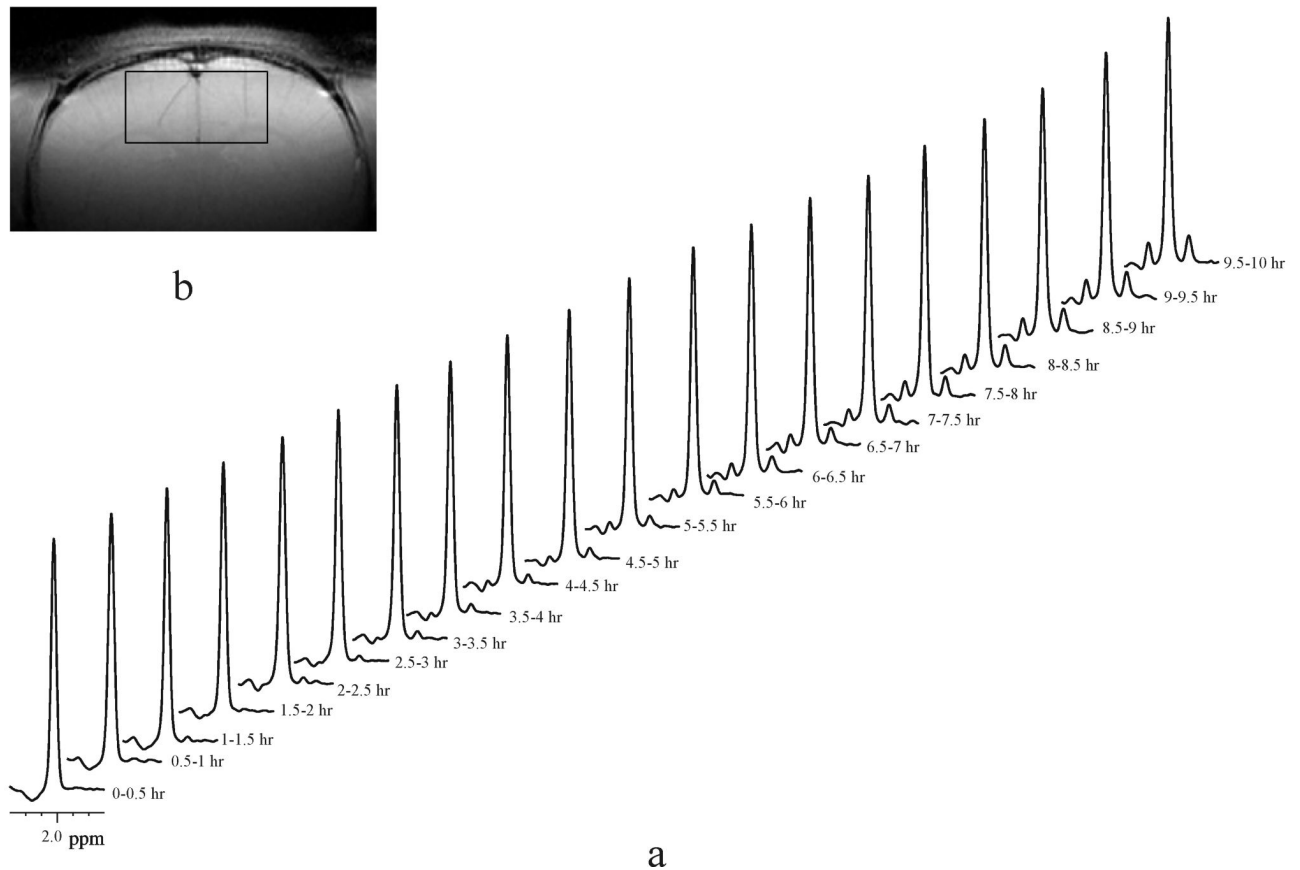


**Fig. 3.** Detection of dynamic  $^{13}\text{C}$ -label incorporation into the *N*-acetyl methyl group of NAA ( $^1J_{\text{CH}} = 128 \text{ Hz}$ ) resonance using a proton-only MRS method at 11.7 Tesla. (a) Each spectrum ( $l_b = -1 \text{ Hz}$ ,  $g_b = 0.005$ ) was an accumulation of 24 minutes ( $\text{NA} = 440$ ) during a 10-hour  $[\text{U-}^{13}\text{C}]$  glucose infusion. The stack of spectra were acquired from a  $6 \times 3 \times 6 \text{ mm}^3$  ( $108 \mu\text{L}$ ) voxel in an individual rat brain. (b) The coronal image shows the location of the measured spectroscopic volume (slice thickness = 1 mm, field of view = 2.56 cm, matrix size =  $256 \times 256$ , TR/TE = 1000/10 ms, number of averages = 2).

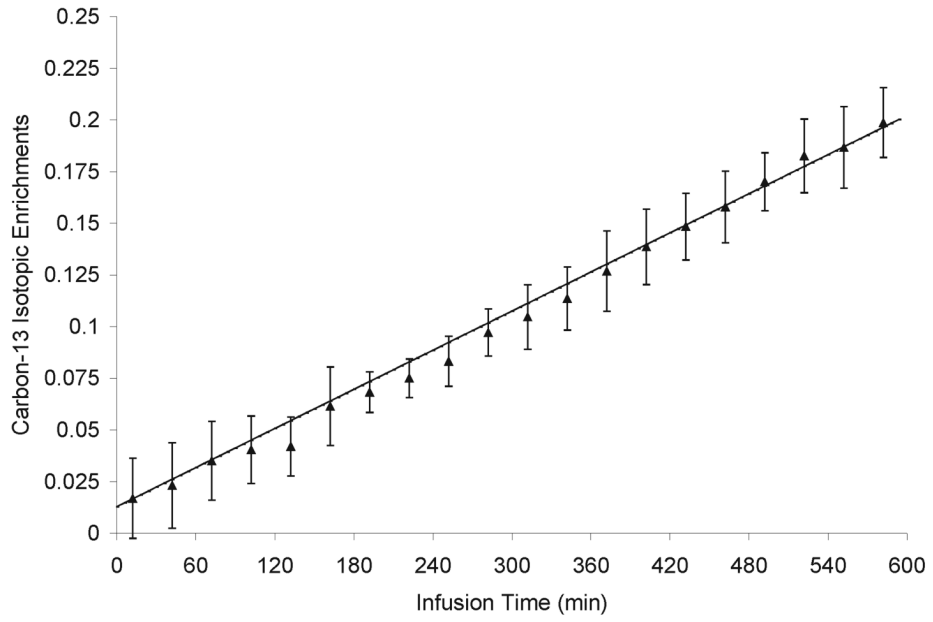


**Fig. 4.**  $^{13}\text{C}$  labeling time course of the *N*-acetyl methyl group of NAA and fitting to the linear model. Data were averaged from twelve rats. Error bars =  $\pm 1$  standard deviation.